Mechatronics and Automation Technology
J. Xu (Ed.)

doi:10.3233/ATDE241270

Future-Driven Computational Modeling: Shaping the Next Era of Electroplating

Ilhem BOUTANA[a,1], Oussama BOULTIF[b], Abdessalam ZAIT[b]
[a] *Laboratory of Electrical Engineering and Industrial Electronics, Faculty of Science and Technology, University of Jijel, Jijel, Algeria*
[b] *Electrical Engineering Department, University of Jijel, Jijel, Algeria*

Abstract. Electroforming is a manufacturing process that uses electrolysis to deposit metal onto a substrate, creating intricate metal components with exceptional precision. Commonly used in industries like jewelry, electronics, aerospace, and automotive, it excels in producing complex geometries and high-precision parts. Modeling electroforming simulates the physical and chemical interactions during metal deposition to optimize parameters and improve product quality. This study uses a 2D, time-dependent secondary current distribution model in COMSOL Multiphysics to validate copper and nickel electroforming, offering insights into process optimization and performance prediction.

Keywords. Electroforming, electrodeposition, electroplating.

1. Introduction

Electrochemical forming, known as electroforming, has gained significant recognition as a sustainable additive manufacturing process, leveraging electrochemical principles to construct structures in a layer-by-layer fashion [1-3]. This technique is extensively utilized in the fabrication of complex components for diverse applications, (e.g., printing, holography, and sound reproduction). In particular, the aerospace industry relies heavily on components made from nickel and its alloys, which are produced through electroforming. Despite its broad industrial adoption, the academic and scientific community’s attention to electroforming remains limited, creating challenges in advancing the technology toward fully automated production systems (e.g., [4,5]).

Electroforming, is a fabrication process for components through electrodeposition, with a fundamentally straightforward mechanism. The required metal is deposited onto a die submerged in a suitable electrolyte until it reaches a thickness sufficient for the structure to be self-supporting. The removal of the die effectively completes the production of the electroform. The die is shaped and finished to the required specifications, and while there may be minimal adhesion between the deposited metal and the die, the surface contour and finish of the die are precisely replicated on the contact surface of the electroform.

---

[1] Corresponding Author, Ilhem BOUTANA, Laboratory of Electrical Engineering and Industrial Electronics, Faculty of Science and Technology, University of Jijel, Jijel, Algeria; E-mail: hafsaoui@univ-jijel.dz.

The interest in simulating the electroforming process is not a recent development. The first numerical studies of the process emerged in the 1970s. Since then, electroforming has been studied only sporadically, despite the rapid advancements in computer science. However, interest in the process, its applications, and its potential for more rigorous modeling has significantly increased over the past decade (e.g., [6-12]). Electroforming, in particular, involves changes in the shape of the reaction surface, and modeling these changes can be challenging. Meanwhile, experimental studies of this process have been conducted more systematically, providing data that facilitate the development of modeling tools. This underscores the importance of numerical modeling for electroforming, which allows for the simulation of various experimental operations in this technology, a key objective of our work.

Following these considerations, this paper is a short paper of our previous work [13], where we presented in detail our innovative approach of numerically modeling the electroforming processes. This research aims to develop a 2D, time-dependent secondary current distribution model in COMSOL Multiphysics to simulate the electroforming of copper and nickel, enabling performance prediction and process optimization. The study enhances the understanding of electroforming's physical and chemical interactions and offers validated numerical assessments for the electroplating process. It highlights the potential industrial applications, including PCBs, aerospace, and automotive manufacturing, improving both efficiency and precision.

2. Related Work

In this Section, we provide an overview of state-of-the-art Electroforming proposals.

In [14], the authors advance the understanding of nickel electroforming by scaling up from lab-scale experiments to industrial applications, specifically focusing on the electroforming of a mechanical vane—a critical component in the aerospace industry. By utilizing a 3D secondary current distribution model developed in COMSOL Multiphysics, they successfully simulate the electroforming process, achieving results that align with experimental findings conducted in an industrial pilot tank. The study demonstrates the model's ability to predict thickness distribution under various current densities and highlights its application for both quantitative and qualitative studies depending on operational conditions. Furthermore, the investigation into the electroformed surface characteristics, supported by scanning electron microscopy, provides insights into the microstructure and growth mechanisms of the nickel deposits.

In [15], a sustainable method for recovering high-purity copper from waste printed circuit boards (WPCBs) is proposed. The study introduces ethanol as a dispersant in the flotation process, significantly enhancing the efficiency of copper extraction from WPCBs. Following this, electrodeposition is employed to recover pure copper from the concentrated material. Key parameters, including the solid-to-liquid ratio and applied voltage, are optimized to achieve a high copper deposition rate while preserving deposit purity. This research advances both resource recovery and environmental sustainability by offering an effective, environmentally friendly approach to WPCB recycling.

[16] Explores the use of pulse-reverse electrodeposition to fabricate Nickel (Ni) coatings reinforced with different carbon allotropes, including Carbon Nanotubes (CNT), Graphite (Gt), and Graphene (Gr). The authors investigate the impact of these carbon inclusions on the microstructural and electrochemical properties of the coatings. Various characterization techniques, such as Field-Emission Scanning Electron Microscopy,

Atomic Force Microscopy, X-ray diffraction, and Raman spectroscopy, reveal that the addition of carbon allotropes enhances the structural uniformity and reduces surface roughness, with Ni-Gr showing the lowest roughness. Electrochemical studies using Electrochemical Impedance Spectroscopy and polarization tests demonstrate significant improvements in corrosion resistance, with Ni-Gr coatings achieving up to 60% better protection compared to pure Ni coatings. The reduction in corrosion current density further confirms the superior protective performance of the Ni-Gr composite coating.

3. Numerical Modeling of Electroforming Process

In this Section, we present an overview of the numerical modeling of Electroforming processes along with the mathematical models used in our numerical evaluation.

Electroforming is a complex and widely utilized technique for fabricating microstructured components. Its nature is multiphysical, as it encompasses fluid dynamics, ion concentration, electric current distribution, and other interrelated physical phenomena. Therefore, modeling this process requires a deep understanding of the physical phenomena involved, along with expertise in mathematical modeling and a rigorous study with well-defined assumptions.

3.1. Mathematical Models

The electroforming process is modeled under conditions where PH=4, indicating a low proton concentration relative to the concentrations of other ions. As a result, the material balance for protons is not required in the model. It is assumed that deposition at the cathode and dissolution at the anode occur with 100% current efficiency, excluding the possibility of any secondary reactions.

During the process, differences in electrolyte density develop within the closed cell, leading to a higher density at the anode than at the cathode. Although this could induce free convection within the cell, the effect is considered negligible due to minimal variations in composition. Consequently, the Nernst-Planck equation [17] is employed to describe the movement of ions within the electrolyte shown in equation (1).

$$N_i = -D_i \nabla c_i - z_i u_i F c_i \nabla \phi_i \tag{1}$$

Where N_i Is the transport vector, D_i represents the diffusion coefficient, c_i is the concentration of i ions in the electrolyte, z_i is the charge for ionic species, u_i is the mobility of loaded species i, ϕ_i the potential in the electrolyte, and F is the Faraday constant defined as $F = 96485{,}338$ [C/mol].

Moreover, the material balances are expressed by equation (2). However, for each species $i = 1.2$, the criterion of electrical neutrality is stated by equation (3):

$$\frac{\partial c_i}{\partial t} + \nabla . N_i = 0 \tag{2}$$

and:

$$\sum_i z_i c_i = 0 \tag{3}$$

On the other hand, the boundary conditions at the anode and cathode are defined by the Butler-Volmer equation [18] presented in equation (4).

$$i_{ct} = i_0 \left(e^{\frac{\alpha_{a,m} F.\eta}{RT}} - \frac{c_m}{c_{m,ref}} e^{\frac{-\alpha_{c,m} F.\eta}{RT}} \right) \tag{4}$$

Where i_{ct} is the local charge transfer current density, i_0 is the exchange current density, $\alpha_{a,m}$ is the anode charge transfer coefficient, $\alpha_{c,m}$ is the cathode charge transfer coefficient, R is the universal gas constant (i.e., $8.314\ \mathrm{J/mol.K}$), T is the temperature at which the problem is studied, c_m is the concentration of the metal in the solution, $c_{m,ref}$ is the reference concentration of the metal, and η is the activation overpotential, defined as follows:

$$\eta = \phi_{s,0} - \phi_l - \Delta\phi_{eq} \tag{5}$$

Such that $\phi_{s,0}$ is the electric potential of the respective electrode, ϕ_l is the potential in the electrolyte, and $\Delta\phi_{eq}$ is the difference between the metal and electrolyte potentials.

3.2. Electroplating Process

The electroplating process involves forming a metallic coating on a solid substrate through the reduction of metal cations using a continuous electric current. In this setup, the part to be coated serves as the cathode in an electrolytic cell, while the electrolyte consists of a metal salt solution, and the anode is typically either a block of the same metal or an inert conductive material. The external power supply drives the current through the system.

This model incorporates a secondary current distribution and employs full Butler-Volmer kinetics to describe both the metal deposition at the cathode and dissolution at the anode. The anode undergoes dissolution, while the cathode, often coated with a metal such as nickel, receives the deposited metal. The model calculates the thickness of the deposited layer on the cathode and the current efficiency, with the overpotential for the electrode reaction at index m defined by the following equation.

$$\eta_m = \phi_{s,0} - \phi_l - E_{eq,m} \tag{6}$$

where $E_{eq,m}$ is the difference between the metal and electrolyte potentials at the surface of the electrode, measured at equilibrium using a common reference potential.

$$i_{loc,Ni} = i_{0,Ni} \left(e^{\frac{\alpha_a F.\eta_{Ni}}{RT}} - e^{\frac{-\alpha_c F.\eta_{Ni}}{RT}} \right) \tag{7}$$

4. Preliminary Evaluation and Assessment

In this Section, we present our numerical evaluation and assessment conducted using the Electroforming process. Specifically, we address the modeling of the electroplating process.

This evaluation concerns electroplating, a widely used technology for numerous technological applications, ranging from decorative coatings to high-precision passive electromagnetic shielding devices. This electroplating model employs a secondary current distribution in conjunction with full Butler-Volmer kinetics (see equation (7)) to accurately represent the metal deposition process at the cathode and the dissolution reaction at the anode. A concurrent hydrogen evolution reaction is also present at the cathode. The thickness of the deposited layer at the cathode is calculated along with the current efficiency. The 2D model geometry, illustrated in figure 1, represents a microstructure component with small dimensions. The anode is a flat-dissolving cube surrounding a cubic piece, which acts as the cathode to be coated with a metal plating.

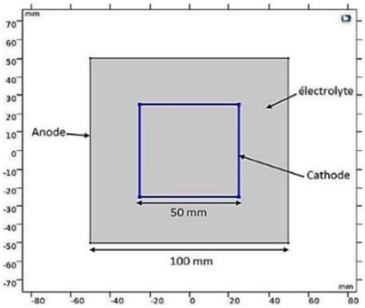

Figure 1. 2D Geometric Model for Electroplating Application.

Moreover, the conductivity of the metal in the anode and cathode is much higher than that of the electrolyte, and the electric potential in the metal is assumed to be constant. Therefore, variations in the activation overpotential are due to the electrolyte potential at the electrode surfaces. Based on these assumptions, the electrodes are treated as boundaries in the simulation.

It should be noted that the numerical results obtained for a 2D electroplating application are theoretically consistent. Indeed, in figure 2(a), we observe a predictable distribution of electrolyte potential that corresponds to the shape of the electrodes, decreasing from the anode to the cathode. As for the electrolyte current density vectors, they are directed from the anode to the cathode, with a noticeable concentration at the corners of the cathode due to the tip effect. Figure 2(b) shows the thickness of the deposited layer after 24h ($t = 86400s$) of deposition. We observe a uniform deposition of nickel on all sides of the cube, which is explained by the uniformity of the current density. However, the thickness variations at the corners are relatively significant, with a factor of 4 compared to the flat surfaces, which can be well explained by the tip effect.

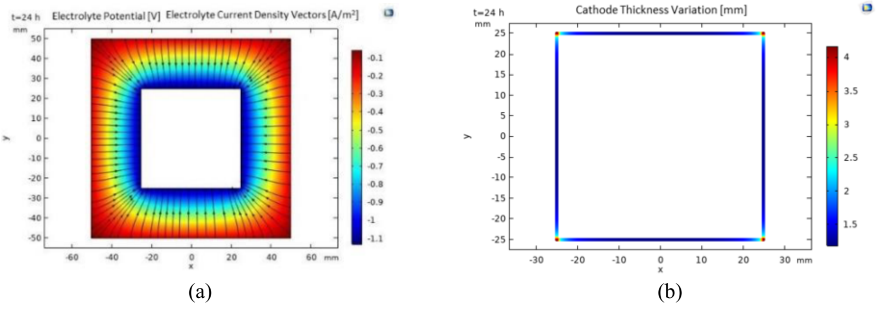

(a) (b)

Figure 2. Electrolyte Potential, Electrolyte Current Density Vectors (a) – Total Variation in Cathode Thickness after $t = 24H$ (b)

In another study, we attempted to develop a 3D electroplating model that involves the electroplating of a small ring centered in an electrolyte, considered the cathodic electrode, surrounded by a cylindrical anode (see figure 3(a)). The numerical results obtained for this application allow for the same observations regarding the potential and electrolyte current density vectors as in the previous study (see figure 3(b)).

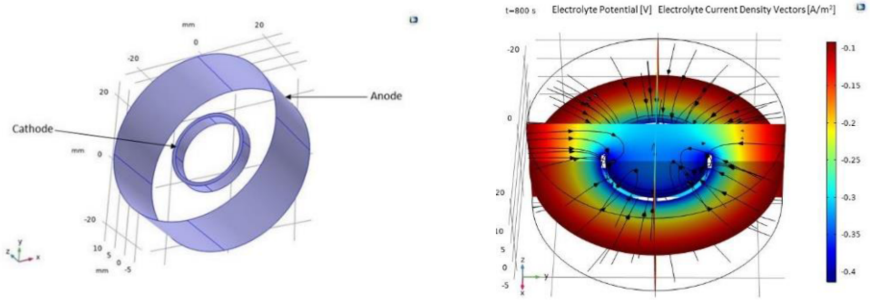

(a) (b)

Figure 3. 3D Electroplating Geometric Model of Ring (a) – Electrolyte Potential, Electrolyte Current Density Vectors (b).

Figure 4 illustrates the thickness of the deposited layer after 800 seconds of deposition. The results reveal considerable variation in layer thickness, with differences exceeding a factor of three between the inner and outer regions of the ring. Furthermore, the maximum deposition is observed at the edges of the ring. These findings indicate that improvements in the cell geometry are necessary to achieve a more uniform deposition across the surface.

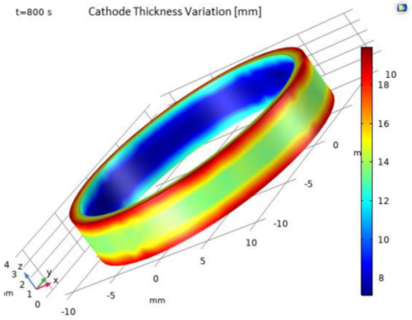

Figure 4. Total Variation in Cathode Thickness.

5. Conclusions and Future Work

Electroforming is a promising technique for producing complex and high-quality components with growing potential across various industries. This study focused on numerical modeling component shaping, especially surface treatment, using the electroplating process. The results were theoretically validated and aligned well with findings from experimental studies. Future work could involve developing models for more complex geometries and exploring other emerging trends in the electroforming process (e.g., [19-23]).

References

[1] Rai, P.K., Gupta, A. Electroforming Process for Microsystems Fabrication[J]. Journal of The Electrochemical Society, 2023, 170(12), art. 123510.

[2] Behagh, A.M., Tehrani, A.F. Investigation and Modelling of Copper Electroforming Process for Surface Roughness Parameters using Regression and Pareto Anova Analyses[J]. Surface Engineering and Applied Electrochemistry, 2023, 59(6), pp. 780-790.

[3] Biswal, H.J., Kaur, J.J., Vundavilli, P.R., Gupta, A. Recent Advances in Energy Field Assisted Hybrid Electrodeposition and Electroforming Processes[J]. CIRP Journal of Manufacturing Science and Technology, 2022, 38, pp. 518–546.

[4] Syamsuir, S., Susetyo, F.B., Soegijono, B., et al. Rotating-magnetic-field Assisted Electrodeposition of Copper for Ambulance Medical Equipment. Automotive Experiences, 2023, 6(2), pp. 290–302.

[5] Jamesh, M., Kumar, S., Narayanan, T.S. Electrodeposition of Hydroxyapatite Coating on Magnesium for Biomedical Applications[J]. Journal of Coatings Technology and Research, 2012, 9, pp. 495–502.

[6] Bali, H., Hafsaoui, I., Makhlouf, B. A Simultaneous Resolution Method for Coupling Field Circuit Equations for Steady-State Skin Effect Problems[C]. IEEE International Conference on Electrical Sciences and Technologies in Maghreb, 2018, pp. 1-6.

[7] Boutana, I., Mekideche, M.R., Bali, H. Analysis Model and Numerical Investigation of Electromagnetic Tube Expansion with Field Concentrator[C]. The 20th IEEE International Multi-Conference on Systems, Signals & Devices, 2023, pp. 294-298.

[8] Boutana, I., Bouferroum, S.E., Laouira, A. Modeling of the Innovative Magnetic Pulse Joining Technology[C]. The 19th IEEE International Multi-Conference on Systems, Signals & Devices, 2022, pp. 2115-2120.

[9] Boutana, I., Bahloul, A., Boukendir, S. Numerical Investigation on Weldability of Workpieces using Magnetic Pulse Welding Process[C]. IEEE International Conference on Design & Test of Integrated Micro & Nano-Systems, 2021, pp. 1-6.

[10] Boutana, I., Boussalem, M.E., Laouira, A., Bouferroum, S. 3D Modelling of the Mechanical Behaviour of Magnetic Forming Systems[J]. Bulletin of Electrical Engineering and Informatics, 2022, 11(4), pp. 1807-1817.

[11] Boutana, I., Bousba, A., Benhadj, Y.N. Numerical Modeling of Industrial Parts Manufacturing using Electromagnetic Hemming Process[J]. The International Journal of Advanced Manufacturing Technology 133, 2024, pp. 1943-1959.

[12] Boutana, I., Mekideche, M.R. Finite Element Model Analyzing Dynamical Behavior of Sheet Electromagnetic Forming[C]. The 6th IEEE International Multi-Conference on Systems, Signals and Devices, 2009, pp. 1-6.

[13] Boutana, I., Boultif, O., Zait, A. Next-Gen Computational Modeling for Transformative Electroforming Processes[J]. Journal of Machine Intelligence and Data Science 5, 2024, pp. 104-118.

[14] Andreou, E., Roy, S. Modelling and Verification of the Nickel Electroforming Process of a Mechanical Vane Fit for Industry 4.0[J]. Digital Chemical Engineering, art, 2024, 100177.

[15] Li, Y., Wei, X., Liu, H., Sun, Y. Flotation Assisted Electrodeposition Process to Recover Copper from Waste Printed Circuit Boards[J]. Chemical Engineering Journal, art, 2024, 154747.

[16] Akbarpour, M.R., Fathi, M., Gharibi Asl, F., Kim, H.S. Effects of Carbon Allotrope Type on Microstructural and Electrochemical Properties of Ni-C Nanocomposite Coating Prepared by Pulse-Reverse Electrodeposition Method[J]. Metals and Materials International, 2024, pp. 1-11, 2024.

[17] Maexa, R. Nernst-Planck Equation". In: Encyclopedia of Computational Neuroscience[J]. Springe, 2022, pp. 2182–2187.

[18] Dickinson, E. J., Wain, A.J. The Butler-Volmer Equation in Electrochemical Theory: Origins, Value, and Practical Application[J]. Journal of Electroanalytical Chemistry, 2020, 872, art. 114145.

[19] Wang, Y., Wang, H., Chen, X., et al. Self-Learning Effect of Csfamapbibr Memristor Achieved by Electroforming Process[J]. Materials Chemistry and Physics. 2023, 310, art. 128488.

[20] Son, S., Torre, C.L., Kindsmuller, A., et al. A Study of the Electroforming Process in 1t1r Memory Arrays[J]. IEEE Transactions on Computer-Aided Design of Integrated Circuits and Systems, 2023, 42(2), pp. 558-568.

[21] Wang, H., Xing, J., Fan, T., et al. An Effect of Layered Auxiliary Cathode on Thickness Uniformity in Micro Electroforming Process[J]. Micromachines, 14(7), art. 1307.

[22] Setiawan, J., Sudiarso, A., Winursitoc, I., et al. Influence of Concentration of Copper Electrolyte, Voltage, and Time of Electroforming on Conductive Acrylonitrile Butadiene Styrene Parts on Deposition Rate and Microstructure[J]. International Journal of Engineering, 2024, 37(10), pp. 1914-1925.

[23] Zhang, Y., Ming, P., Zhang, X., et al. Jet Electroforming of High-Aspectratio Microcomponents by Periodically Lifting a Necked-Entrance through-mask[J]. Micromachines, 2024, 15(6), art. 753.